Scripta Materialia 194 (2021) 113646

Contents lists available at ScienceDirect

Scripta Materialia

journal homepage: www.elsevier.com/locate/scriptamat

Local atomic configuration approach to the nonmonotonic concentration dependence of magnetic properties of $Ni_2Mn_{1+x}Z_{1-x}$ (Z = In,Sn,Sb) Heusler alloys

Karol Załęski[a,*], Marcus Ekholm[b], Björn Alling[b], Igor A. Abrikosov[b,c], Janusz Dubowik[d]

[a] NanoBioMedical Centre, Adam Mickiewicz University, ul. Wszechnicy Piastowskiej 3, Poznań 61-614, Poland
[b] Department of Physics, Chemistry and Biology, Linköping University, SE-58183, Sweden
[c] Materials Modeling and Development Laboratory, National University of Science and Technology "MISIS", Moscow, 119049, Russia
[d] Institute of Molecular Physics, Polish Academy of Sciences, ul. Smoluchowskiego 17, 60-179 Poznań, Poland

ARTICLE INFO

Article history:
Received 24 April 2020
Revised 19 November 2020
Accepted 20 November 2020
Available online 4 December 2020

Keywords:
Heusler phases
Ferromagnetic shape memory alloy
Magnetic thin films
Magnetic structure
Ab initio calculation

ABSTRACT

The $Ni_2Mn_{1+x}Z_{1-x}$ Heusler alloys, where Z = In, Sn,Sb are attractive candidates for shape memory applications. The effect is directly related to their magnetic properties. We have studied these systems by ab-initio calculations and experiments, focusing on magnetic moments and exchange-bias fields. The calculations indicate that the composition dependence of the total magnetic moment is due to competing ferromagnetic and antiferromagnetic alignment between Mn atoms on different sublattices and with different local environments. This phenomenon can also explain the composition dependence of the exchange-bias effect.

Heusler alloys constitute a family of materials with numerous interesting properties [1], such as half-metallicity, magnetocaloric and magnetic shape memory effects, which are related to their magnetic properties. Some of the most spectacular effects, like the giant exchange-bias (EB) [2] and inverse magnetocaloric effects [3], low Gilbert damping [4], or shell-ferromagnetism [5], are observed in off-stoichiometric Heusler alloys. In such cases, the coexistence of domains with different local environments of the atoms, and the interaction between them, play a major role.

In this work, we study magnetic properties in the Heusler alloys $Ni_2Mn_{1+x}Z_{1-x}$ (Z = In,Sn,Sb). These alloys are interesting candidates for shape memory applications [1]. Application of a magnetic field induces a structural transformation from an antiferromagnetic (AFM) martensite phase to a ferromagnetic (FM) cubic austenite phase [1]. This effect depends strongly on the difference in the magnetization of the phases, which is higher in the cubic austenite phase [6,7].

The magnetization of these alloys have been studied experimentally by Ito et al. as a function of the alloy composition. The crystal structure of the austenite phase, shown in Fig. 1, can be viewed as four interpenetrating *fcc* (face centered cubic) sublattices, where X$\in$ ($\frac{1}{4}$, $\frac{1}{4}$, $\frac{1}{4}$) and ($\frac{3}{4}$, $\frac{3}{4}$, $\frac{3}{4}$), Y$\in$(0,0,0) and Z$\in$($\frac{1}{2}$, $\frac{1}{2}$, $\frac{1}{2}$). These sublattices are occupied as X = Ni, Y = Mn and Z = In/Sn/Sb. By substituting a fraction of the Z-atoms with Mn atoms, a qualitative difference in total magnetic moment (M_{tot}) vs composition (x) was observed in the $Ni_2Mn_{1+x}Z_{1-x}$ systems [8,9], as shown in Fig. 1. Increasing the Mn content in the Z = In system leads to a monotonic increase of M_{tot}. However, the trend is opposite for the Z = Sb system, with a monotonous decrease of M_{tot}. An interesting intermediate situation is found for Z = Sn, where the concentration dependence has a nonmonotonic character, with a minimum at about $x = 0.2$.

The role of magnetic interactions between Mn atoms occupying two different sublattices in cubic Ni-Mn-based Heusler alloys has been studied in previous works. Sokolovskiy et al. investigated by ab-initio calculations the influence of chemical disorder on magnetic properties of $Ni_2Mn_{1+x}Sn_{1-x}$ alloys [10], but they could not confirm the non-monotonic behavior of $M_{tot}(x)$. In the theoretical work of Entel et al., the interactions between the spins on the original Y-sublattice (Mn_Y) and on the Z-sublattice (Mn_Z) or on the X-sublattice (Mn_X) in Ni–Mn–Z alloys where shown to have exclusively antiferromagnetic character [11]. This can not explain nonmonotonic behavior of the $M_{tot}(x)$. Recently, Cavazzini et al. reported on the influence of Sn composition on the magnetic properties of cubic austenite $Ni_{1.92}Mn_{1.44}In_{0.64-x}Sn_x$ alloys [12]. They examined two magnetic states, where the alignment of Mn mo-

* Corresponding author.
E-mail address: zaleski@amu.edu.pl (K. Załęski).

https://doi.org/10.1016/j.scriptamat.2020.113646
1359-6462/

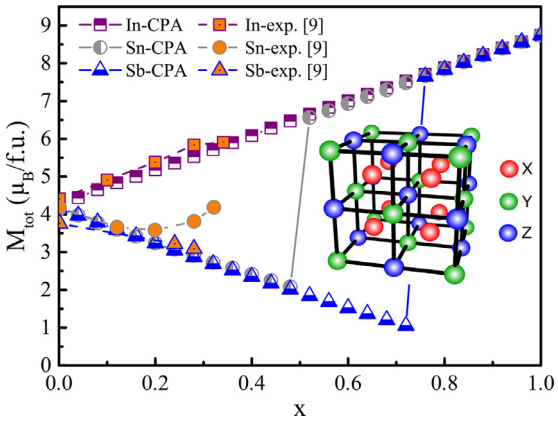

Fig. 1. Magnetic moment (in Bohr magneton per formula unit) obtained by CPA calculations compared with experiment (Ref. [9]). Inset - $L2_1$ crystal structure of Ni_2MnZ Heusler alloys.

ments on the Y and Z sublattices were either completely ferromagnetic or antiferromagentic. In the In-rich case, the calculations fit the experimental values, where the Mn_Z atoms were ferromagnetic. However, in the case of the Sn-rich alloys, neither completely ferromagnetic nor antiferromagnetic configurations did fit the experiment, suggesting the need of a third approach.

In this work we present results from ab-initio calculations and experiments to investigate the origins of these different behaviors in the cubic austenite phase. We also present measurements of the exchange-bias effect for the $Ni_2Mn_{1+x}Sn_{1-x}$ alloy at several compositions of the cubic phase. We show that the presence of competing FM and AFM can explain the concentration dependence of the magnetization for $Ni_2Mn_{1+x}Sn_{1-x}$ alloys. Simultaneously, our model correctly describes $Ni_2Mn_{1+x}In_{1-x}$ and $Ni_2Mn_{1+x}Sb_{1-x}$ alloys.

We have performed ab-initio calculations for $Ni_2Mn_{1+x}Z_{1-x}$ (Z = In,Sn,Sb) using the exact muffin-tin orbitals (EMTO) method [13–15] with the Perdew-Burke-Ernzerhof exchange-correlation functional [16]. In order to model the alloy system, one may use large supercells [17–19] to create a unique local environment for each atom. However, this approach may turn out very time consuming, and we have employed an alternative route, the Coherent Potential Approximation (CPA) [20]. In the framework of the CPA one replaces each atom in the alloy by an effective atoms with scattering properties determined self-consistently. This allows the size of the simulated system to be reduced to a single unit cell, although all local fluctuations of the composition and spin orientation are averaged out [21]. We used a basis of s, p, d, f muffin-tin orbitals to expand the Kohn-Sham orbitals. To sample the Brillouin zone, we used a $21 \times 21 \times 21$ k-point mesh from which 946 points were chosen by a Monkhorst-Pack routine for the irreducible part of the Brillouin zone. Total energy was converged within 0.1 μRy during the self-consistency cycles. We used a semi-elliptical contour in the complex energy plane with 32 energy points spanning 2.5 Ry below the Fermi level, which included the 4*d* states of the Z atom.

Epitaxial thin films with $x = 0, 0.2, 0.36$ were sputter deposited on MgO(001) substrates. Details on the preparation, structural and magnetic properties of thin films can be found in Supplementary Materials.

In Fig. 1 we show the magnetic moment of the cubic $L2_1$-$Ni_2Mn_{1+x}Z_{1-x}$ alloys as obtained with the CPA applied to the Z-sublattice, compared with the experimental data in Ref. [9]. For all systems, the magnetic moments of the Mn atoms at the Y-sublattice are coupled ferromagnetically to each other. In the $Ni_2Mn_{1+x}In_{1-x}$ alloys, we find the Mn_Z atom to align its magnetic moment in parallel to the total magnetic moment (FM coupling) at all compositions. Increase of concentration then translates to an increase of the total magnetic moment, which reproduces the available experimental data well. For the case Z = Sb, the decrease of the magnetic moment is captured as well. However, the non-monotonic behavior for Z = Sn is not reproduced. Nevertheless, we do observe how the magnetization of the Mn_Z atoms are reversed at high concentrations. This indicates the presence of competing FM and AFM interactions in the alloys, which are not properly accounted for by the single-site CPA. We therefore extend our model to include disorder of the local Mn_Z moments.

In order to allow for magnetic disorder, we turn to the partially disordered local moment (PDLM) approximation [22] to model a random mixture of $Mn_Z^{\uparrow}$ and $Mn_Z^{\downarrow}$ atoms on the Z-sublattice. The chemical formula of the sublattice is then expanded to read $Z_{1-x}(Mn^{\uparrow}{}_{\xi}Mn^{\downarrow}{}_{1-\xi})_x$, where $0 \leq \xi \leq 1$ is the concentration of $Mn_Z{}^{\uparrow}$ atoms. An FM configuration corresponds to $\xi = 1$, while $\xi = 0.5$ corresponds to an equal mixture of $Mn_Z^{\uparrow}$ and $Mn_Z{}^{\downarrow}$, which represents a completely disordered magnetic state. At $\xi = 0$, all Mn_Z are antiferromagnetically aligned to the Mn atoms on the Y-sublattice.

We then need to determine the appropriate value of ξ for each composition, x. Total energy calculations for different values of ξ and x yield a minimum for Mn_Z in either FM ($\xi = 1$) or AFM ($\xi = 0$) configuration, as shown in Fig. 2, since they correspond to the magnetically ordered model. In order to take the disorder into account we therefore represent the nearest neighbor shell of the Mn_Z atoms as a statistical distribution of cuboctahedrons, populated by $0 \leq n \leq 12$ Mn_Z atoms, illustrated Fig. 3(a). The magnetic configuration of the Mn_Z atoms in the nearest neighbor shell is then allowed to vary as a function of n. The statistical weight of each cuboctahedron in the model is given by the probalility, P, of finding a cuboctahedron containing n Mn_Z atoms, and can be written as: [23]

$$P(n,x) = \frac{N!}{(N-n)!n!}(1-x)^{N-n}x^n, \tag{1}$$

where $N = 12$ is the number of sites in a cuboctahedron. This probability function is plotted as a function of composition in Fig. 3(b), for various values of n. Eq. (1) and its modifications are commonly used to calculate the distribution of the local atomic configurations determined by the nuclear magnetic resonance spin-echo measurements [24,25].

We calculate the magnetic configuration of the Mn_Z atoms by CPA, treating the Z sublattice as a homogenous mixture of Mn_Z and Z atoms, with the concentration $x = n/12$. For Z = In we find FM alignment for all values of n. In the case of Z = Sn the orientation is FM for $n \geq 6$, and for Z = Sb when $n \geq 9$. We may now sum up the probability, S, of finding a cuboctahedron with FM-aligned Mn_Z atoms, as follows: $S^{\mathrm{In}}(x) = \sum_{n=0}^{12} P(n,x)$, $S^{\mathrm{Sn}}(x) = \sum_{n=6}^{12} P(n,x)$, $S^{\mathrm{Sb}}(x) = \sum_{n=9}^{12} P(n,x)$. The total probability, S, is used as the PDLM order parameter by setting $S = \xi$ so that the Z sublattice is modelled as:

$$Z_{1-x}(Mn_S^{\uparrow}Mn_{1-S}^{\downarrow})_x. \tag{2}$$

The values of S^Z are plotted as a function of the concentration x in Fig. 3(b).

Fig. 4 (a) presents the concentration dependence of the experimental [9] (full symbols) and calculated (half-open symbols) total magnetic moments of the cubic $Ni_2Mn_{1+x}Z_{1-x}$ (Z = In,Sn,Sb) alloys, where the Z sublattice is modelled based on Eq. (2). For Z = In, $\xi = 1$ at all compositions, meaning that we correctly recover the linear concentration dependence.

In contrast, for Z = Sn we reproduce a nonlinear concentration dependence of the magnetization. For low x the M_{tot} decreases, reaching a minimum, followed by an increase up to the maximum

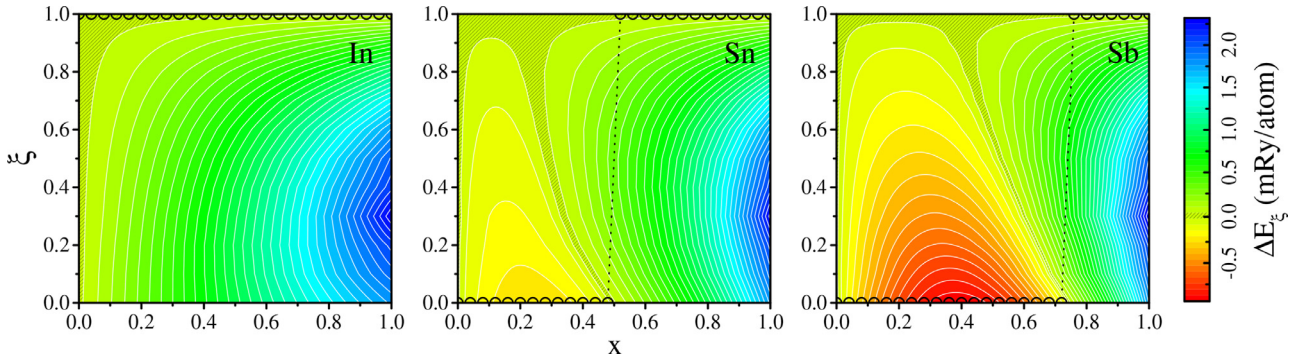

Fig. 2. Total energy calculated for $Ni_2Mn_{1+x}Z_{1-x}$ alloys (Z = In,Sn,Sb) as a function of composition, x, and magnetic state, ξ. The energy scale is relative to the FM state ($\xi = 1$). The lowest energy is represented by "○" symbols.

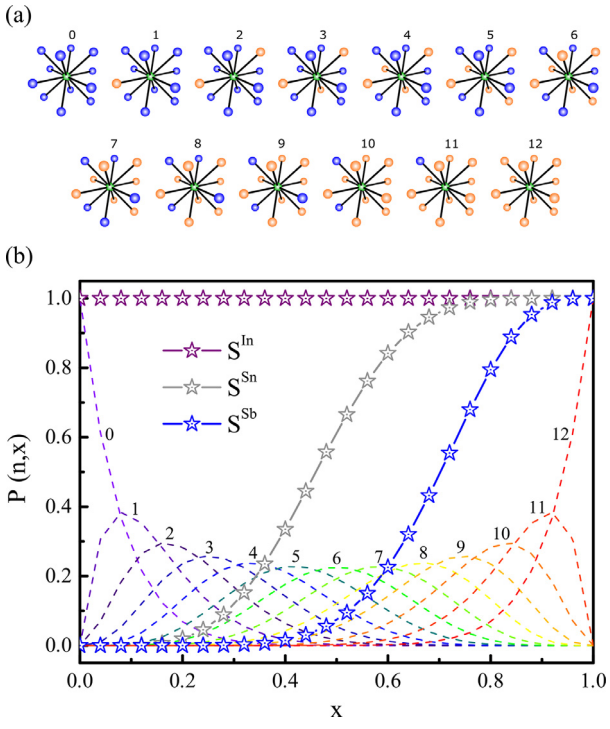

Fig. 3. (a) Atomic configurations used to represent the $Ni_2Mn_{1+x}Z_{1-x}$ alloys in the probability distribution $P(n, x)$. The number n of Mn_Z atoms (orange) on the Z-sublattice is related to the alloy composition as $x = n/12$. (b) $P(n, x)$ calculated from Eq. (1), corresponding to cuboctahedrons populated by n Mn_Z atoms. The star symbols denote the total probability, $S^Z(x)$, of cuboctahedrons with FM-aligned Mn_Z atoms.

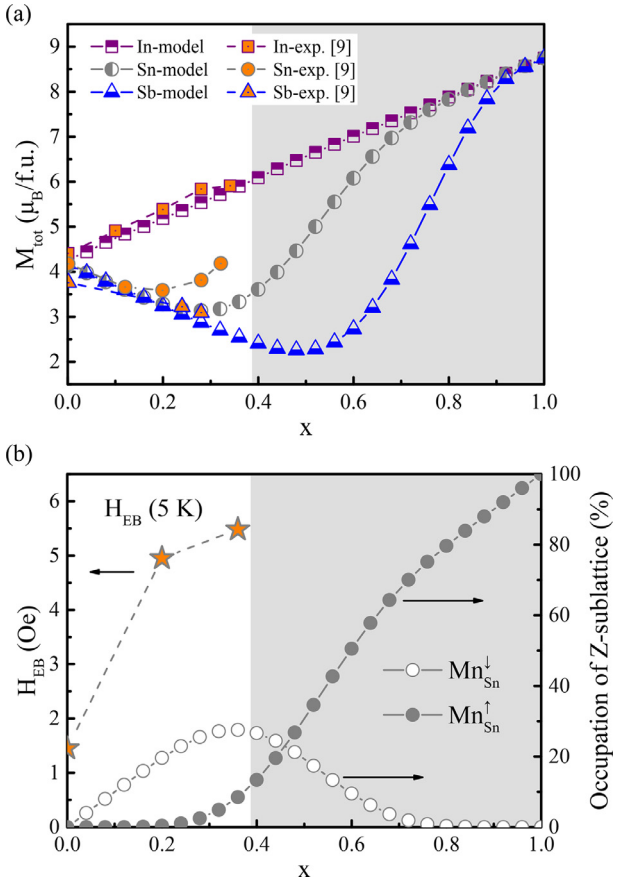

Fig. 4. (a) Total magnetic moment M_{tot} of $Ni_2Mn_{1+x}Z_{1-x}$ alloys (Z = In,Sn,Sb). The experimental [9] and calculated data are shown by solid and half-open symbols, respectively. The non-shaded part of the plot corresponds to the $L2_1$ phase stability composition range. (b) The occupation level of Z(Sn)-sublattice by Mn atoms with FM (closed symbols) and AFM (open symbols) spin orientation in $Ni_2Mn_{1+x}Sn_{1-x}$. The star symbols represent the H_{EB} measured at 5 K for $Ni_2Mn_{1+x}Sn_{1-x}$ ($x = 0, 0.2, 0.36$) thin films.

value, which is reached for the Ni-Mn compound. The minimum of the calculated curve is found at higher values of x than in the experimental data. The quantitative disagreement is likely because of a higher concentration of Mn atoms on the Z sublattice in the real alloys. This is due to metastability and tendency to phase decomposition of Z = Sn alloys [26], which could be more likely with increasing Mn composition [27]. Therefore, one can expect a slightly higher concentration of FM-aligned Mn_Z atoms in the real alloys. In fact, the phase separation and the existence of FM and AFM clusters in Ni-Mn-Sn alloys were comprehensively studied in Refs. [28], where the authors concluded that the upturn in the total magnetization is determined by the presence of nanoscale magnetic phase separation into FM and AFM regions. Our results demonstrate that the effect is intrinsic for the considered alloys, and it should be seen in $Ni_2Mn_{1+x}Sn_{1-x}$ samples without any additional thermal treatment aimed at phase decomposition.

For the case of Z = Sb, we reproduce the linear decrease of $M_{tot}(x)$ with concentration, in line with the available experimental data. We also observe a nonmonotonic concentration dependence at higher values of x. It is associated with a more stable AFM coupling between Mn and Mn_Z atoms in the Z = Sb alloy. A similar effect is observed in the austenite phase of Ni-Mn-Ga magnetic shape memory alloys [29,30].

A suggestion for the reason behind this effect is the change in the electronic density of state (DOS) as the concentration of Mn_Z atoms changes in the studied alloys (Figs. S17-S19 in Supplemen-

tary Materials). In the FM state, as the concentration of Mn_Z increases, there is a transfer of the spectral weight of the spin up peak located between −0.1 and −0.05 Ry below the Fermi energy from higher to lower energy. In the antiferromagnetic configuration, the DOS is virtually unaffected. Thus, increasing concentration of Mn_Z should shift the energy balance in favor of the FM state.

The coexistence of interacting FM and AFM domains leads to the exchange-bias (EB) effect [2,31,32]. The magnitude of EB can be determined by a shift of the hysteresis loop (H_{EB}) (Figs. S3-S4 in Supplementary Materials). We have therefore measured H_{EB} in $Ni_2Mn_{1+x}Sn_{1-x}$ thin films at low temperature (5 K).

The results are shown in Fig. 4b. In the stoichiometric case, $x = 0$, H_{EB} is almost zero. H_{EB} then increases significantly at higher concentrations to the level of 5 Oe. In the light of our theoretical calculations, we may explain these experimental results as follows (see Figs. S5–S8 in Supplementary Materials). Since the Y-sublattice is fully occupied by the FM oriented Mn atoms, while the Z-sublattice is only partially occupied by the AFM oriented Mn atoms, the FM phase can be considered as a matrix. Therefore, the EB effect, and hence, the magnitude of H_{EB}, should depend on the number of AFM domains. The measurements may be compared to the calculated occupation level of the Z-sublattice by Mn up/down atoms. As the occupancy of Mn on the Z-sublattice increases, the fraction of FM coupled Mn_Z atoms increases monotonically, while the fraction of AFM coupled Mn_Z atoms has a non-monotonic behavior. The maximum fraction of AFM-Mn_Z atoms is reached at the composition $x = 0.36$. At increasing Mn content, the fraction of AFM coupled Mn atoms on the Sn-sublattice decreases. The calculated composition of $Mn^{\downarrow}_{Sn}$ matches the measured H_{EB} relatively well.

In summary, we have carried out experiments and ab-initio calculations for $Ni_2Mn_{1+x}Z_{1-x}$ (Z = In,Sn,Sb) alloys. We find that the composition dependence of the total magnetization can be qualitatively explained with a simple statistical model which includes Mn atoms with both FM and AFM orientations. Our model correctly reproduces the experimentally reported trends of increasing magnetization for $Ni_2Mn_{1+x}In_{1-x}$ and decreasing magnetization for $Ni_2Mn_{1+x}Sb_{1-x}$, with increasing Mn content.

For $Ni_2Mn_{1+x}Sn_{1-x}$ we also reproduce the nonmonotonic composition dependence, which indicates that competing FM and AFM Mn atoms are responsible. This is also supported by measurements of the exchange-bias field in thin films of $Ni_2Mn_{1+x}Sn_{1-x}$, which also seem to support the notion of competing FM and AFM interactions.

It should be noted that our computational model only takes into account the mixture of FM and AFM Mn atoms in a mean-field sense. It does not explicitly include local environment effects, such as magnetic and structural short-range order or lattice relaxations. A continuation of our work would be supercell calculations to include such effects, in order to improve the quantitative agreement. Nevertheless, the qualitative success of our simple model indicates that it captures the most important physical effect in these alloys: that of competing FM and AFM interactions.

Declaration of Competing Interest

The authors declare that they have no known competing financial interests or personal relationships that could have appeared to influence the work reported in this paper.

Acknowledgments

This research was supported by the Polish National Science Centre grant DEC-2014/15/B/ST3/02927. In addition, we acknowledge support form the Strategic Research Areas the Swedish e-Science Research Centre (SeRC) and Advanced Functional Materials at Linköping University (Faculty Grant SFOMatLiU No. 2009 00971). Analysis of theoretical data was supported by the Ministry of Science and Higher Education of the Russian Federation in the framework of Increase Competitiveness Program of NUST “MISIS” (No K2-2019-001) implemented by a governmental decree dated 16 March 2013, No 211. The calculations were performed on resources provided by the Swedish National Infrastructure for Computing (SNIC) at the National Supercomputer Centre (NSC), Linköping University, Sweden.

Supplementary material

Supplementary material associated with this article can be found, in the online version, at 10.1016/j.scriptamat.2020.113646

References

[1] T. Graf, C. Felser, S.S. Parkin, Prog. Solid State Chem. 39 (1) (2011) 1–50, doi:10.1016/j.progsolidstchem.2011.02.001.
[2] A.K. Nayak, M. Nicklas, S. Chadov, P. Khuntia, C. Shekhar, A. Kalache, M. Baenitz, Y. Skourski, V.K. Guduru, A. Puri, U. Zeitler, J.M.D. Coey, C. Felser, Nat. Mater. 14 (2015) 679, doi:10.1038/nmat4248.
[3] T. Krenke, E. Duman, M. Acet, E.F. Wassermann, X. Moya, L. Mañosa, A. Planes, Nat. Mater. 4 (2005) 450, doi:10.1038/nmat1395.
[4] A. Bonda, L. Uba, K. Załęski, S. Uba, Phys. Rev. B 99 (2019) 184424, doi:10.1103/PhysRevB.99.184424.
[5] A. Çakır, M. Acet, M. Farle, Sci. Rep. 6 (2016) 28931.
[6] T. Krenke, M. Acet, E.F. Wassermann, X. Moya, L. Mañosa, A. Planes, Phys. Rev. B 72 (2005) 014412, doi:10.1103/PhysRevB.72.014412.
[7] T. Krenke, M. Acet, E.F. Wassermann, X. Moya, L. Mañosa, A. Planes, Phys. Rev. B 73 (2006) 174413, doi:10.1103/PhysRevB.73.174413.
[8] W. Ito, X. Xu, R.Y. Umetsu, T. Kanomata, K. Ishida, R. Kainuma, Appl. Phys. Lett. 97 (24) (2010) 242512, doi:10.1063/1.3525168.
[9] W. Ito, X. Xu, R.Y. Umetsu, T. Kanomata, K. Ishida, R. Kainuma, J. Appl. Phys. 109 (7) (2011) 07A926, doi:10.1063/1.3556708.
[10] V.V. Sokolovskiy, V.D. Buchelnikov, M.A. Zagrebin, P. Entel, S. Sahoo, M. Ogura, Phys. Rev. B 86 (2012) 134418, doi:10.1103/PhysRevB.86.134418.
[11] P. Entel, M.E. Gruner, S. Fähler, M. Acet, A. Çahir, R. Arróyave, S. Sahoo, T.C. Duong, A. Talapatra, L. Sandratskii, S. Mankowsky, T. Gottschall, O. Gutfleisch, P. Lázpita, V.A. Chernenko, J.M. Barandiaran, V.V. Sokolovskiy, V.D. Buchelnikov, Phys. Status Solidi (b) 255(2) 1700296. 10.1002/pssb.201700296
[12] G. Cavazzini, F. Cugini, M. Gruner, C. Bennati, L. Righi, S. Fabbrici, F. Albertini, M. Solzi, Scr. Mater. 170 (2019) 48–51, doi:10.1016/j.scriptamat.2019.05.027.
[13] L. Vitos, Computational Quantum Mechanics for Materials Engineers - The EMTO Method and Applications, Springer-Verlag London Limited, 2007.
[14] L. Vitos, Phys. Rev. B 64 (2001) 014107, doi:10.1103/PhysRevB.64.014107.
[15] L. Vitos, I.A. Abrikosov, B. Johansson, Phys. Rev. Lett. 87 (2001) 156401, doi:10.1103/PhysRevLett.87.156401.
[16] J.P. Perdew, K. Burke, M. Ernzerhof, Phys. Rev. Lett. 77 (1996) 3865–3868, doi:10.1103/PhysRevLett.77.3865.
[17] B. Alling, S. Shallcross, I.A. Abrikosov, Phys. Rev. B 73 (2006) 064418, doi:10.1103/PhysRevB.73.064418.
[18] B. Alling, M. Ekholm, I.A. Abrikosov, Phys. Rev. B 77 (2008) 144414, doi:10.1103/PhysRevB.77.144414.
[19] M. Ekholm, P. Larsson, B. Alling, U. Helmersson, I.A. Abrikosov, J. Appl. Phys. 108 (9) (2010) 093712, doi:10.1063/1.3476282.
[20] A.V. Ruban, I.A. Abrikosov, Rep. Prog. Phys. 71 (4) (2008) 046501.
[21] J. Faulkner, Prog. Mater. Sci. 27 (1 - 2) (1982) 1–187, doi:10.1016/0079-6425(82)90005-6.
[22] M. Ekholm, H. Zapolsky, A.V. Ruban, I. Vernyhora, D. Ledue, I.A. Abrikosov, Phys. Rev. Lett. 105 (2010) 167208, doi:10.1103/PhysRevLett.105.167208.
[23] H.A.M. de Gronckel, W.J.M. de Jonge, in: R.E.W. L. H. Bennett (Ed.), Magnetic Multilayers, World Scientific Publishing Co. Pte. Ltd., 1994, pp. 111–145.
[24] S. Wurmehl, J.T. Kohlhepp, H.J.M. Swagten, B. Koopmans, J. Appl. Phys. 111 (4) (2012) 043903, doi:10.1063/1.3684686.
[25] S. Wurmehl, J.T. Kohlhepp, H.J.M. Swagten, B. Koopmans, M. Wójcik, B. Balke, C.G.F. Blum, V. Ksenofontov, G.H. Fecher, C. Felser, Appl. Phys. Lett. 91 (5) (2007) 052506, doi:10.1063/1.2760158.
[26] W.M. Yuhasz, D.L. Schlagel, Q. Xing, K.W. Dennis, R.W. McCallum, T.A. Lograsso, J. Appl. Phys. 105 (7) (2009) 07A921, doi:10.1063/1.3067855.
[27] W. Yuhasz, D. Schlagel, Q. Xing, R. McCallum, T. Lograsso, J. Alloys Compd. 492 (1) (2010) 681–684, doi:10.1016/j.jallcom.2009.12.016.
[28] S. Yuan, P.L. Kuhns, A.P. Reyes, J.S. Brooks, M.J.R. Hoch, V. Srivastava, R.D. James, C. Leighton, Phys. Rev. B 93 (2016) 094425, doi:10.1103/PhysRevB.93.094425.
[29] P.J. Brown, A.Y. Bargawi, J. Crangle, K.-U. Neumann, K.R.A. Ziebeck, J. Phys. 11 (24) (1999) 4715–4722, doi:10.1088/0953-8984/11/24/312.
[30] P. Lázpita, J.M. Barandiarán, J. Gutiérrez, C. Mondelli, A. Sozinov, V.A. Chernenko, Phys. Rev. Lett. 119 (2017) 155701.
[31] J. Dubowik, I. Gościańska, K. Załęski, H. Głowiński, A. Ehresmann, J. Appl. Phys. 113 (2013) 193907.
[32] S. Giri, M. Patra, S. Majumdar, J. Phys. Condens. Matter 23 (7) (2011) 073201.